Journal of Volcanology and Geothermal Research 263 (2013) 42–57

Contents lists available at ScienceDirect

Journal of Volcanology and Geothermal Research

journal homepage: www.elsevier.com/locate/jvolgeores

Recent eruptions at Bezymianny volcano—A seismological comparison

Michael E. West

Geophysical Institute, University of Alaska Fairbanks, Fairbanks, AK 99775, United States

ARTICLE INFO

Article history:
Received 15 May 2012
Accepted 22 December 2012
Available online 31 December 2012

Keywords:
Seismology
Volcano seismology
Volcanic eruptions
Arc volcanoes
Bezymianny
Kamchatka

ABSTRACT

For the past few decades, Bezymianny volcano has erupted once to twice per year. Here, I examine eight eruptive events between 2006 and 2010. This is the first time period for which proximal or broadband seismic data have been recorded at Bezymianny. Several recurring patterns are demonstrated in advance of eruptions. Eruptions are generally preceded by 12–36 h of tremor energy elevated by 2 to 3 orders of magnitude. Locatable earthquake activity is quite erratic in the days before eruptions. For eruptions of juvenile magma, however, the cumulative moment magnitude increases with the repose time since the previous eruption. Though tenuous, this relationship is statistically significant and could improve forecasts of Bezymianny eruptions. The most energetic eruptions demonstrate increasing multiplet activity in the run-up, followed by a rapid cessation at the time of eruption. When present, this behavior marks increasing pressure in the conduit system as degassing eclipses the capacity for venting. Very long period seismicity (>20 s periods) accompanies some eruptions. These tend to be the same short-lived high-energy eruptions that exhibit multiplet precursors. Four eruptions are examined in detail to illustrate the variety in eruption mechanisms. Lava dome collapses, sustained eruptions, singular paroxysmal explosions and post-explosion lava flows occur in different combinations demonstrating that more than one eruption trigger is regulating Bezymianny. Compared to Bezymianny's fifty-year modern history, recent eruptions have been shorter-lived and separated by longer repose times. Some evidence suggests that these eruptions may be increasingly explosive—a speculation that carries significant hazard implications. If true, however, this threat is tempered by solid evidence that the most explosive eruptions are preceded by the clearest precursors, suggesting an ability to improve the already excellent eruption forecasts available for Bezymianny.

1. Introduction

In the decade from 2000 to 2010, Bezymianny volcano had approximately 17 independent eruptions that were large enough to generate pyroclastic flows stretching several kilometers and put ash thousands of meters into the atmosphere (Senyukov et al., 2004; Girina, 2013). These eruptions were significant enough to warrant public safety notifications. The location of Bezymianny, on Russia's Kamchatka peninsula, poses significant hazards to trans-Pacific aircraft routes (Neal et al., 2009). Prevailing weather patterns sweep atmospheric ash eastward over the north Pacific (Schneider et al., 2000; Ramsey and Dehn, 2004). Eruptions in the past decade have regularly resulted in air traffic restrictions (e.g., Neal et al., 2009; McGimsey et al., 2011; Neal et al., 2011). Most of these were short-lived singular eruptions that, broadly speaking, appear similar to one another.

There is no single standard for measuring the size of a volcanic eruption. However, the majority of Bezymianny eruptions during this decade were assigned a volcanic explosivity index (VEI) (Newhall and Self, 1982) of 2 or 3 by the Smithsonian Global Volcanism Program (Venzke et al., 2012). Senyukov et al. (2004) have documented a common set of seismic and ground temperature observations that precede most of these eruptions. The repeatability of the precursory pattern has allowed many of the eruptions to be accurately forecast on the scale of days to hours, often with increasingly precise time windows (Senyukov, 2006). The author is unaware of a series of comparably sized eruptions with an equivalent forecasting success.

Bezymianny has been erupting intermittently since its initial historic eruption in 1956. During the VEI 5 eruption, the southeast flank collapsed concurrent with a massive lateral blast that erupted a combined volume of more than 3 km^3 of material and left a 700 m deep crater (Bogoyavlenskaya et al., 1985). The resulting horseshoe-shaped crater was 1.5 by 2.8 km in diameter. Subsequent eruptions have built a dome that now fills in much of this crater. For an overview of the 1956 eruption and ensuing activity see Gorshkov (1959), Bogoyavlenskaya et al. (1991) and Girina (2013). This eruption preceded the strikingly similar 1980 eruption of Mt. St. Helens by 24 years and is frequently considered the type example of sector collapse and lateral blast volcanism (Voight et al., 1981; Belousov et al., 2007). Though Bezymianny was only lightly instrumented during its first 50 years of recovery, the eruption record has been well documented through field observations, photographs and petrologic sampling. Because Bezymianny has rebuilt much of its edifice in just 50 years, it is an ideal place to examine how volcanoes respond, long-term, to massive sector collapse events.

E-mail address: mewest@alaska.edu.

0377-0273/$ – see front matter © 2013 Elsevier B.V. All rights reserved.
http://dx.doi.org/10.1016/j.jvolgeores.2012.12.015

The first two decades following the 1956 eruption were characterized by magma extrusion accompanied occasionally by modest explosions. At times, spines of solid magma were extruded. At other times, the extruded products were more plastic. By 1976, the dome had reached a height of more than 800 m (Bogoyavlenskaya et al., 1985 and references therein). Beginning in 1977, the number of explosive eruptions began to increase. The duration of individual eruptions, on average, decreased as well. These eruptions have often been preceded and or followed by lava extrusion. There is evidence of solid magma spines being extruded prior to some eruptions (Malyshev, 2000). And several eruptions have been followed by viscous lava flows emplaced over the course of days (Carter et al., 2007). However, the extrusive periods have generally been short lived. If the first twenty years of eruption can be described as continuous effusive eruption with occasional lulls and explosions, the post-1977 era should be described as quiescence punctuated by discrete eruptions.

This activity is represented schematically in Fig. 1. Based on the growth of the dome, the rate of magma production was clearly very high in initial years and remained elevated during the first two decades. Once the dome was large, a significant portion of the eruption products began spilling out of the crater making it challenging to quantify magma production with existing data. As well, the volume of magma deposited as tephra remains largely unquantified. As a result, this model is purely qualitative. Even without constraints on the actual magma production rate, several features are likely robust: the high rate of magma production in the initial years; the dominantly extrusive phase; the transition to dominantly explosive phase; and the variability in recent eruption/extrusion sequences. When the top of the volcano was removed in 1956, the conduit system was effectively shortened by a kilometer when more than a cubic kilometer of overburden was removed. Any equilibrium that might have existed in the magmatic system was destroyed. The ensuing years of dome growth and punctuated extrusion are compatible with this model. Though several mechanisms might ultimately be driving eruption (e.g., second boiling, crustal relaxation, new magma from the deep crust), all of these eruption sources could be accelerated and sustained by unloading. Likewise, the slowed growth in recent decades is plausibly due to the fact that Bezymianny is closing in on its pre-1956 topography. Regardless of mechanism, the eruption behavior of Bezymianny has evolved steadily over the past half century.

Several lines of evidence suggest that the dome is a significant factor in regulating eruptions. Increases in surface temperature in the days to weeks prior to eruption are large enough to be observed with satellite remote sensing (Ramsey and Dehn, 2004). The rate of rockfalls on the dome increases similarly on a scale of days to weeks (Senyukov et al., 2004). The observations of magma spines extruded prior to eruption are anecdotal, but appear to have occurred on several occasions (Girina, 2013). Significant ground deformations have not been reported concurrent with eruptions other than the 1956 one, though it should be noted that deformation data has only recently become available. The fact that recent explosive eruptions typically last minutes, and not hours, suggests that the eruption source is shallow and quickly exhausted. Together these

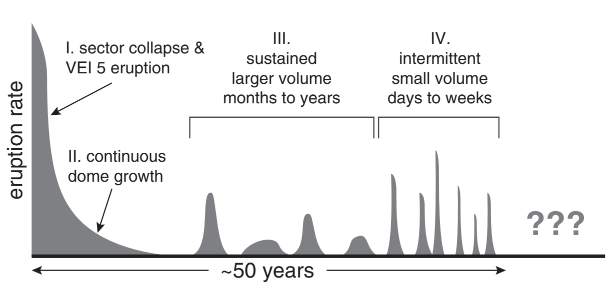

Fig. 1. Conceptual timeline of eruption activity at Bezymianny in the 50 years following the 1956 eruption.

observations imply that the dome acts as a cap on the volcanic system and plays an essential role in regulating eruptions.

Other evidence suggests a strong role for a crustal magma reservoir kilometers below the surface. Whole rock chemistry has evolved gradually but consistently since 1956. Linear compositional trends through time (including SiO_2, Al_2O_3, K_2O, Na_2O) suggest a homogenizing reservoir that provides a consistent source of magma. Geophysical evidence for crustal magma storage is scant. But a modest curtain of seismicity does suggest the possibility of magma storage at about 3 km below sea level. Seismic evidence from multiplet earthquakes suggests that at least one recent eruption sourced material from deep enough to disrupt the conduit system beneath the edifice (Thelen et al., 2010a). Lastly, the regularity of eruptions is striking. It is hard to conceptualize this regularity without invoking some type of steady inexorable driving process from below.

The goal of this study is to identify the features of the Bezymianny system that have regulated recent eruptions. There are many common features that suggest a repeatable eruption mechanism. Closer inspection however demonstrates a range of eruption triggers. By identifying the triggers for recent eruptions, and particularly the role of the dome, it becomes feasible to speculate about future activity in light of the model in Fig. 1. Significant geophysical instrumentation at Bezymianny, paired with repeated field observations and sampling, makes these objectives reasonable. In this paper, I focus on eruptions for which seismic data is available within 15 km of the volcano. Such data exists for 2006 and beyond.

2. Data

2.1. The PIRE project

Bezymianny volcano has been the centerpiece of a several-year multi-disciplinary project led by a collaboration of U.S. and Russian scientists. The project was focused on comparisons between recent sector collapse volcanoes with an emphasis on Bezymianny and Mt. St. Helens. Though Bezymianny has been known internationally for decades, political realities limited the involvement of foreign scientists until the 1990s. Even today, the logistical consequences of this history are felt by most researchers working in Kamchatka. The PIRE project (funded under the National Science Foundation's Partnership for International Research and Education program) sought to build an international research focus on Bezymianny while equipping young scientists with the skills to work in Kamchatka and similar environments.

Despite political isolation, one organization has had an ongoing presence at Bezymianny throughout its 20th century history. The Institute of Volcanology and Seismology (IVS), part of the eastern branch of the Russian Academy of Sciences, has coordinated research and monitoring at Bezymianny from its first signs of unrest in 1955 through today (e.g., Gorshkov, 1959; Bogoyavlenskaya et al., 1991). Beginning in 1999, the Klyuchevskoy group of volcanoes, of which Bezymianny is part, was installed with a seismic network and real time telemetry to IVS in Petropavlovsk-Kamchatsky. Since this time, the Kamchatka Branch of Geophysical Services (KBGS) has carried out real time seismic monitoring and routine earthquake location in the larger vicinity of Bezymianny. In 2005, KBGS was operating six short-period analog seismic stations within 50 km of Bezymianny. The closest stations to Bezymianny, 14 km distant, allowed the most prominent seismic events to be detected, though seismicity at neighboring volcanoes often masked activity. As part of the PIRE project, KBGS and U.S. collaborators undertook an effort to provide seismic coverage specific to Bezymianny. This network would provide greater sensitivity to Bezymianny seismicity, depth control on earthquake locations, broadband coverage to characterize the full spectrum of activity and high dynamic range digital recording to avoid issues with clipped data that are common to analog volcano networks.

2.2. Instrumentation

A campaign-style seismic network was installed progressively between 2006 and 2009 (Fig. 2). On-site recording allowed these stations to be placed with minimal power needs and without consideration of telemetry. Equipment was furnished by the IRIS/PASSCAL instrument center. All stations were broadband Guralp CMG-3T seismometers (120 s) except for BEZB and BEZC (Guralp 40T, 30 s) and BEZD (Streickheisen STS-2, 120 s). Digitizing and acquisition were performed with Quanterra Q330 dataloggers. All data was sampled at 100 samples per second. In most cases, these stations were visited just once per year. Because the subarctic active volcano environment is not conducive to solar power, these stations operated on air cell batteries—a strategy well tested in Alaska. The small footprint of this design allowed stations to be deployed high on the Bezymianny edifice. Four of the stations are within 1 km of the crater rim (the size and activity of the dome preclude any notion of installing stations inside the crater). 14 stations were installed over the course of the project, with as many as 11 operating concurrently (Fig. 2).

2.3. KBGS catalog and instrumentation

In addition to the campaign-style equipment, five new stations were added to the telemetered network (Fig. 2). These short-period analog stations have improved the routine earthquake catalog produced by KBGS, by lowering the magnitude of catalog completeness and improving location errors. The KBGS earthquake catalog for the Klyuchevskoy group of volcanoes is produced using the DIMAS software package (Droznin and Droznina, 2011).

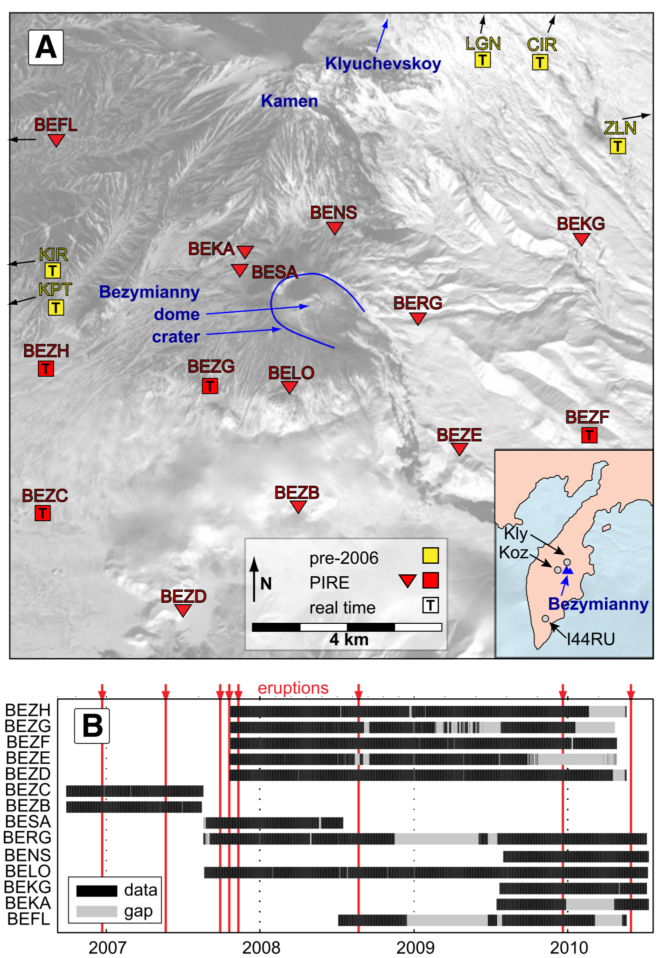

Fig. 2. Map and timeline of seismic stations operated at Bezymianny during the study period. Panel A: map view of PIRE project stations as well as the backbone short-period network in the region. Inset map shows the location of Klyuchi (Kly), Kozyrevsk (Koz) and I44RU on the Kamchatka Peninsula in the Russian Far East. Panel B: timeline of operation for each of the PIRE network stations.
ASTER base map image provided by S. Rose at Univ. Pittsburgh, IVIS Lab.

3. Analysis

Here I focus on eight eruptive episodes between late 2006 and 2010. For brevity, these are referred to as events number 1–8. Table 1 provides the parameters of each event. The selection of these eight is somewhat subjective. However, it includes events that deposited ash over several square kilometers and are separated by weeks or months. In the few instances where explosive activity continued over hours, I treat the event as a singular eruption.

3.1. Tremor

There are several common methods for monitoring the strength of volcanic tremor. RSAM (Endo and Murray, 1991), reduced displacement (Aki and Koyanagi, 1981; van Manen et al., 2010), and seismic energy (Johnson and Aster, 2005; Buurman et al., 2013) are rooted in a common method. All three approaches measure total ground shaking by averaging or summing the complete seismic record or its square. RSAM is the least insightful, though also the least subjective, as it makes no attempt to correct for station characteristics or source location. Reduced displacement and energy both attempt to provide a metric that is independent of station characteristics and distance from the source. This is achieved by making gross assumptions about ground properties and wave propagation. These two techniques provide measures that are comparable across a seismic network and between volcanoes, but only if one admits very significant error bounds. Recent work has pointed out discrepancies in the calculation of reduced displacement between studies (van Manen et al., 2010). For these reasons, I use energy as the tremor measure for Bezymianny. Relative kinetic energy is calculated from the time integral of the particle velocity squared. This is an unambiguous computation. Subjectivity is introduced by extrapolating this to a source energy:

$$E_{\text{source}} = 2\pi r^2 \rho V_p \frac{1}{A} \int U^2 dt \tag{1}$$

where

$$A = \exp(-\pi f r / V_P Q). \tag{2}$$

I use *P*-wave velocity $V_p = 3$ km/s, average density $\rho = 2$ kg/m^3, a predominant frequency $f = 3$ Hz, and an attenuation quality factor $Q = 10$, consistent with comparable environments (e.g., Del Pezzo et al., 2001). r is the distance from the station to the summit vent and U is the velocity seismogram. Johnson and Aster (2005) give a good overview of the caveats on these assumptions. Even so, the estimated seismic energy permits better potential for comparison between volcanoes than RSAM and reduced displacement. When the same station is used to estimate energy at one volcano, most of these terms are invariant. The estimated seismic energy is stable for comparison of Bezymianny eruptions. When comparing to eruption energies at other volcanoes, the estimates have realistic errors of 1–2 orders of magnitude. A final note is that tremor energy calculations assume that all seismic energy is emanating from the volcanic vent. All seismic sources, including seismicity, noise and neighboring volcanoes (in this case, Klyuchevskoy) will contaminate the record. Despite the numerous caveats, however, basic tremor amplitude measures have proven extremely insightful and remain a staple of seismic volcano monitoring (see summary in McNutt and Nishimura, 2008).

Throughout this study, I use station BELO for single station comparisons due to its proximity, quality and continuous operation (Fig. 2). Since BELO was not installed until summer 2007, station BEZB is

Table 1
Eruption parameters.

Eruption	#1	#2	#3	#4	#5	#6	#7	#8
Date and time	2006/12/24 09:17	2007/05/11 14:30	2007/09/25 08:28	2007/10/15 02:23	2007/11/05 08:43	2008/08/19 10:33	2009/12/16 21:46	2010/05/31 12:34
Duration (min)[a]	25	31	18	47	20	26	3	16
Energy (MJ)[b]	1700	740	40	240	1500	1000	12,000	2200
Sudden onset[c]	N	N	N	Y	Y	N	Y	N
Tremor before[d]	Y	N	Y	Y	N	Y	Y	Y
Repose (days)[e]	229	138	137	157	21	288	484	165
CMM before[f]	2.4	–	1.5	2.5	1.2	1.9	2.9	1.6
CMM after[g]	1.9	–	1.7	2.6	2.0	1.8	1.8	1.4
Multiplet termination[h]	Y	–	N	Y	N	?	Y	–
Post-eruption rockfalls[i]	Y	–	N	Y	Y	?	Y	–
Pressure at I44RU (Pa)[j]	–	0.17	–	–	Below noise	–	11	1.5

[a] Duration of the energetic portion of the eruption (Section 3.2).
[b] Energy of the eruption (Sections 3.1 and 3.2).
[c] Determined by visual inspection (Section 3.2).
[d] Based on a ten-fold rise in tremor energy or more during the 24 h preceding the eruption (Section 3.1).
[e] Number of days since the previous eruption.
[f] Cumulative moment magnitude of the located earthquakes in the week prior to eruption (Section 4.1).
[g] Cumulative moment magnitude of the located earthquakes in the week after eruption (Section 4.1).
[h] Subjective assessment based on Fig. 8 of whether the dominant multiplets terminated at the time of eruption.
[i] Based on increase in "long, high frequency" earthquake class in the days following eruption (Fig. 7).
[j] Peak-to-peak infrasound amplitude measured at station 144RU outside Petropavlovsk-Kamchatsky (not shown).

substituted for eruptions number 1 and 2. The reader should keep this discontinuity in mind when comparing data. Stations BELO and BEZB are 1.7 and 4.6 km, respectively, from the center of the dome.

Fig. 3 shows the energy per hour for a time window of nine days around each eruption. Most eruptions show precursory tremor occurring hours to days before the eruption, followed by comparable high energy in the 24 h following eruption. Inspection of the seismic records shows that this tremor comprises a few types. Much of the elevated energy at Bezymianny can be attributed to rockfalls. Rockfall activity on the Bezymianny dome prior to eruptions is well known. Within a kilometer or two of the crater, rockfalls can be heard almost continuously during elevated periods. This is evident in the seismic record from envelopes of energy lasting 5–30 s, rich in frequencies above 3 Hz, with few patterns in particle motion. When this activity is continuous, it is nearly indistinguishable from more classic conduit-sourced tremor. There are however periods of steady tremor that lack the pulsing indicative of discrete rockfalls. This difference can be seen in the scatter in the energy plots (Fig. 3). Eruption 1, for example, is notably rich in rockfalls. This is evidenced in energy by the two orders of magnitude scatter in the days prior to the eruption. A more steady state type of tremor is demonstrated for eruption 8 by the unvarying energies before the eruption.

3.2. Eruption onset, energies and durations

All eight eruptions were relatively short-lived with a clear peak in energy early in the sequence. This makes it straightforward to quantify

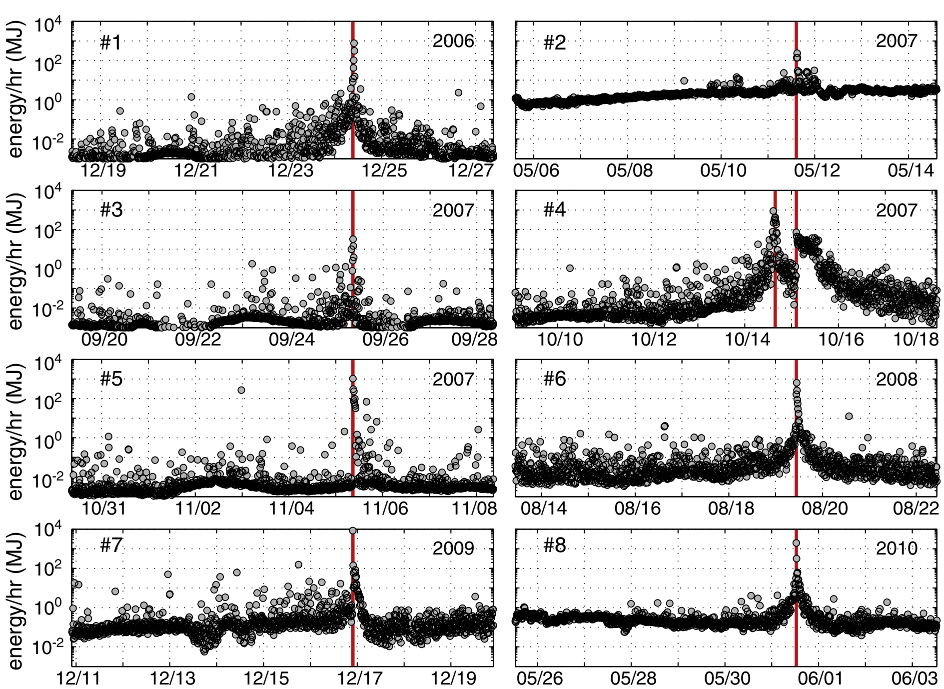

Fig. 3. Tremor amplitude in 9-day windows around each eruption, marked with a red vertical line. Amplitudes are presented as energies assuming a Bezymianny source. See Section 3.1 for details.

energies and durations. Fig. 4 shows 90-minute spectrograms of vertical component data. The eruption onsets follow two styles. I characterize these by visual inspection as either sharp onset or gradual. Sharp onsets can be determined unambiguously to within 1 min. Though subjective, these two styles of eruption onset are relatively clear in the spectrograms. Eruption duration is defined as the time window during which 90% of the seismic energy occurs. The same technique is used to estimate energy as for tremor (Section 3.1) using the square of the norm of the three-component velocity, which is proportional to power. The eruption duration in Table 1 is the amount of time required for the integral of the power to reach 90% of its total value, following Trifunac and Brady (1975). Relative power and duration are estimated using station BELO (BEZB for eruptions 1 and 2).

3.3. Earthquake activity

The routine earthquake catalog produced by KBGS contains about 700 earthquakes at Bezymianny during the 2006–2010 period. These are subset from the larger catalog by requiring a horizontal distance from Bezymianny of less than 7 km and a depth of less than 15 km. These bounds partition the cluster of Bezymianny earthquakes from those under nearby Klyuchevskoy volcano and also exclude the remarkable, though diffuse, cluster of earthquakes that occur in large numbers at 30 km depth. I exclude these since their numbers dwarf the shallow seismicity and it remains unclear to what extent these deep long period earthquakes are directly tied to the Bezymianny and/or Klyuchevskoy systems (George, 2010; Koulakov et al., 2011).

Despite limited historical station coverage at Bezymianny, the KBGS catalog is surprisingly rich in smaller magnitude earthquakes. Though many earthquakes are located using just three stations, all sensors are three-component and P and S phases are picked on all stations. Earthquake size is reported in the KBGS catalog using an energy-based scale (K_s) and not magnitude (Fedotov, 1972). Though K_s is the native unit in this catalog, these values are converted to Richter local magnitude (M_L) here for continuity with other studies. The energy class is converted to magnitude using the expression $M_L = K_s/2 + 0.75$ of Gusev (1991).

The Bezymianny earthquake catalog shows a clear, though variable, relationship to eruptions (Fig. 5). Five eruptions are associated with changes in seismicity. Total earthquake rates are only marginally diagnostic. The sensitivity of the network varies considerably during the four-year period as a result of changing station configuration and periods of eruption at Klyuchevskoy volcano, located 10 km north of Bezymianny. Klyuchevskoy is a basaltic stratovolcano whose eruptions often last months. The effusive nature of these eruptions generates strong tremors that can mask low amplitude seismic signals at Bezymianny for weeks on end. More than half of the earthquakes greater than magnitude 1 occurred within 10 days of an eruption. Seismicity can be high before and/or after eruptions. However, seismicity (>M1) is rarely high outside of an eruption period. The close association with locatable earthquakes underpins the eruption forecasting algorithm that has been used with great success by KBGS (Senyukov, 2006).

3.4. Discrete event detection

Several criteria must be met to reliably constrain an earthquake using traditional travel time-based location techniques: sufficient station coverage; a stable hypocenter inversion; clear *P*-waves; and at least some

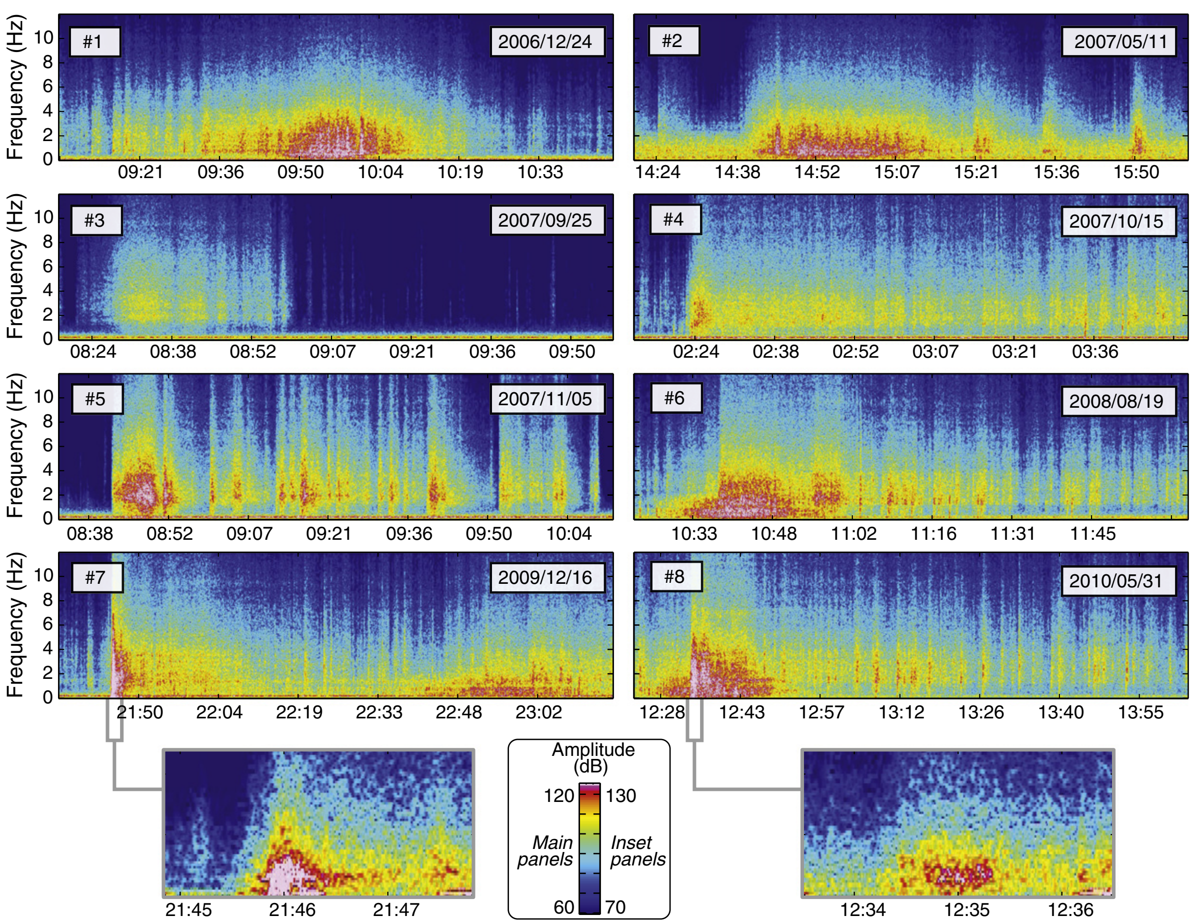

Fig. 4. 90-minute spectrograms of the onset of each eruption. Eruptions start 10 min into each figure. Inset panels show three-minute blowups of eruptions 7 and 8. Data channels are described in the text (Section 3.1).

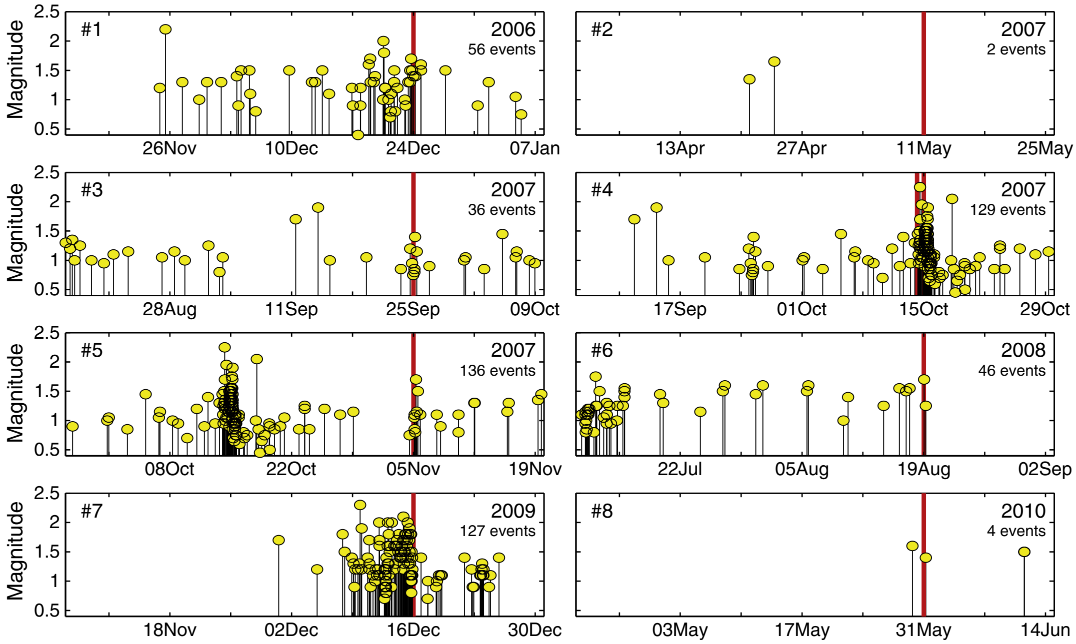

Fig. 5. Earthquakes in 55-day windows around eruptions number 1–8, marked with red vertical lines. Catalog data provided by the Kamchatka Branch of Geophysical Service (KBGS). See Section 3.3 for details.

identifiable *S*-waves. Because these criteria exclude the vast majority of events visible in raw data, we supplement the KBGS earthquake data with a catalog of detected events. The detected events catalog sacrifices the quality of hypocenter solutions to gain a far higher rate of inclusion (e.g., Buurman et al., 2009; Thelen et al., 2011). Since the largest earthquakes are already constrained by the analyst-reviewed catalog, the only sacrifice is in the locations of the smallest events. For time-rate and statistical studies, the detected events catalog offers much improved resolution. The detected events catalog also includes events that lack precise phase arrival times such as rockfalls and low frequency earthquakes. On a practical level, this catalog also offers a way to deal expediently with remote data that is not available until long after a production catalog is completed.

Event detection methods that rely on a single station of data are easily contaminated. The most robust method for filtering out environmental and/or anthropogenic noise is to require events to show across multiple stations. I use the two-step approach laid out by Thompson and West (2010). The first step is event detection on individual data channels. In the second step, these detections are associated across several stations consistent with pre-computed travel times from a grid of test hypocenters. This methodology is essentially the same used by seismic networks worldwide to perform automated earthquake detection. The broad approach is comparable to that used by Thelen et al. (2010a, 2011).

Single channel event detection is performed with a simple short-term average to long-term average ratio. To ensure that all types of discrete events are included, I detect events in both a low and a high frequency band (Table 2). Detections from vertical components are associated across the network by grid searching for hypocenters that fit three or more detection times, assuming *P*-waves. The observed and predicted arrival times must match within 1 s. Detections on horizontal components that fit these solutions are associated as *S*-waves post priori. Three phase arrivals are insufficient to constrain the hypocenter and source time. The grid search technique is still important, however, as it limits the catalog to events with plausible move out across the network. That is, phase arrivals at nearby stations must cluster tightly in time while distal stations must have greater travel times.

Detection and association parameters trade off against one another. Parameters here are based on a separate study in which data from five volcanoes in Alaska were processed using 5760 different combinations of detection and association parameters (Thompson, 2011). The optimal configuration can be qualitatively described as having a lenient detection threshold and relying on strict association criteria. This is demonstrated at Bezymianny by the fact that no more than 30% of the detections from any one channel (vertical) are successfully converted into events. At lower quality stations, this conversion ratio can frequently be less than 1%. While this process can be tuned differently, screening events by requiring them to show on several stations allows the detection criteria to be as inclusive as possible of different event types.

As with any type of catalog, the results reflect changes in the network and background noise. The Bezymianny network evolved considerably during this project (Fig. 2). Fortunately, the configuration was stable within each of the 55-day windows considered here. While the total number of events is strongly influenced by the network and background noise, the trends within these eight windows are robust. Numbers of events vary from 1000 for eruption 2, to 6000 events for eruption 8.

3.5. Event classification

The discrete event catalog contains a wide variety of source types. To characterize these, I estimate the frequency content and duration of each event. Frequency content is summarized by the characteristic frequency, which is defined here as the centroid of the frequency spectrum on the range 0.33–25 Hz. Characteristic frequencies for the complete set of detected events range from 0.6 to 12 Hz with the vast majority of earthquakes falling between 1.5 and 6 Hz.

Event durations are measured as the time window during which 90% of the energy occurs. This is the same approach used for eruption durations (see Section 3.1). The minimum durations are around 2 s. The maximum duration caps artificially near 23 s to minimize overlap

Table 2
Automated event detection parameters.

Frequency band	3–18 Hz	0.5–10 Hz
Short term average window length (STA)	1.4	2.3
Long term average window length (LTA)	7.0	11.5
STA/LTA threshold	3	3

between events close in time. Examination of the full population of durations demonstrates that there are likely few events exceeding this.

Though the classification thresholds are somewhat arbitrary, they produce trends that can be tracked during each eruption and can be used for comparison between eruptions. The distributions vary for each eruption. However, there are recurring clusters in frequency–duration space (Fig. 6A). Based on these clusters, I split the data by frequency above and below a characteristic frequency of 2 Hz. The high frequency category is then split above and below a duration of 10 s. This results in three surprisingly distinct classes of events (Fig. 6). The high-frequency short-duration events have the characteristics of typical volcano-tectonic (VT) earthquakes (McNutt, 2002). The high-frequency long-duration events match the characteristics of rockfalls and block-and-ash flows (DeRoin et al., 2012). The low frequency category likely includes more than one type of event. The shorter duration events may include so-called long period earthquakes thought to be sourced by non-destructive fluid- and/or gas-driven sources (Chouet, 1996). However, there is little seismicity at Bezymianny that is both low in frequency and short in duration. Most low frequency events have durations of more than 10 s. The source of these events is more enigmatic but likely includes spasmodic tremor as well as long period events that have previously been observed to precede rockfalls (Luckett et al., 2008; Thelen et al., 2010a). Fig. 7 shows the rates for each of the event classes by eruption.

3.6. Multiplet seismicity

Multiplet analysis is used to characterize repeatedly occurring earthquakes that produce similar seismic waveforms. Because multiplets are commonly observed at lava domes (e.g., Rowe et al., 2004; Moran et al., 2008; Buurman and West, 2010; Thelen et al., 2011), they are of particular interest at Bezymianny. Multiplet behavior is the pivotal observation in Thelen et al. (2010a) that was used qualitatively to assess the source depth of the Bezymianny eruptions in 2007, referred to herein as events 3–5.

The discrete event detection catalog is used as the input for multiplet analysis. Tests against numerous previous datasets indicate that multiplet results on one station are generally repeatable on other stations in the network so long as the signal to noise ratio remains high. Each of the eight catalogs is a subset for events that have cataloged arrivals on station BELO (BEZB for eruptions 1 and 2). The numbers of events range from 1050 to 4200 for the different 55-day time windows. These traces are bandpass filtered on 0.8–15 Hz and then segmented 1 s before the arrival time and 8 s after. A half-second cosine taper is applied to both ends of the traces. Each trace is cross correlated against each other trace, storing the maximum normalized cross correlation coefficient and its associated lag time. The cross correlation coefficients are the basis for hierarchical clustering. I use a common methodology that assigns events into clusters based on their average correlation coefficient with all other events in the cluster. The choice of 0.8 as the clustering threshold is arbitrary. Examination of the hierarchical cluster trees (not shown) demonstrates that correlation coefficients are distributed smoothly between 0 and 1. A higher correlation threshold will result in more, but smaller, clusters. A lower threshold is more inclusive of events that differ slightly. Because my objective is to determine changes in multiplet activity, I use a relatively high (i.e. strict) threshold for inclusion.

Fig. 8 shows the lifespan of each multiplet that contains five or more events, ordered by date of first appearance, following Thelen et al. (2010a). The number of multiplets varies considerably between eruptions. This variation should be considered cautiously as the detection levels vary significantly between the eight eruption catalogs. The lifespan of the multiplets however is relatively insulated from differences in the underlying catalog.

3.7. Very long period (VLP) seismicity

Explosive volcanism is known to produce seismic waves at periods much longer than typical volcanic earthquake, tremor and rockfall activity. Loosely referred to as VLP (very long period) seismicity (e.g., Arciniega-Ceballos et al., 1999; Chouet et al., 2003; Wiens et al., 2005), this ground motion is best observed at periods beyond the microseism band—periods longer than ~10 s. At these periods, the entire edifice of the volcano is within one wavelength of the source. This ground motion is best conceptualized as short-term deformations of the edifice.

Very long period seismicity is examined at Bezymianny using displacement seismograms low pass filtered at 0.05 Hz. Fig. 9A displays three component VLP records from station BELO. At these frequencies, the background noise is relatively consistent at 2–5 μm. Events 7 and 8 exhibit displacements on the order of 50–200 μm at station BELO. These displacements are large enough to be seen across the network including stations BEZH and BEFL at distances of 6.3 and 8.3 km, respectively (Fig. 9B). These explosions have significant displacements at

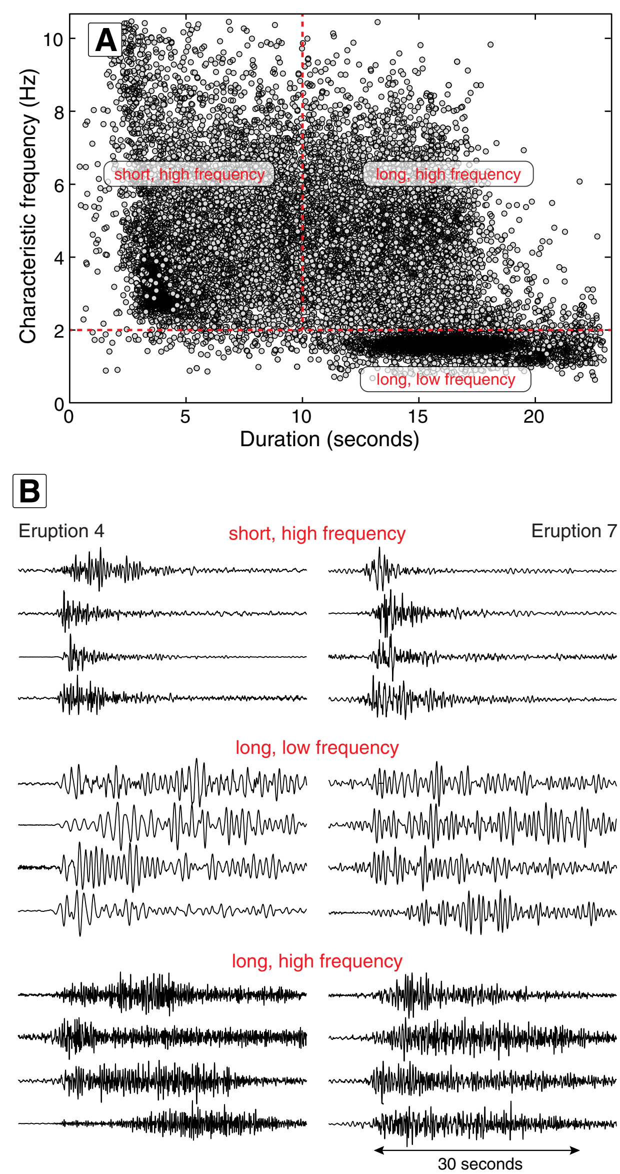

Fig. 6. Earthquakes as a function of frequency and duration using the discrete event detections. Panel A: distribution of events in frequency–distribution space. Panel B: sample waveforms from each event class for two eruptions. Waveforms are drawn from the vertical component of BELO.

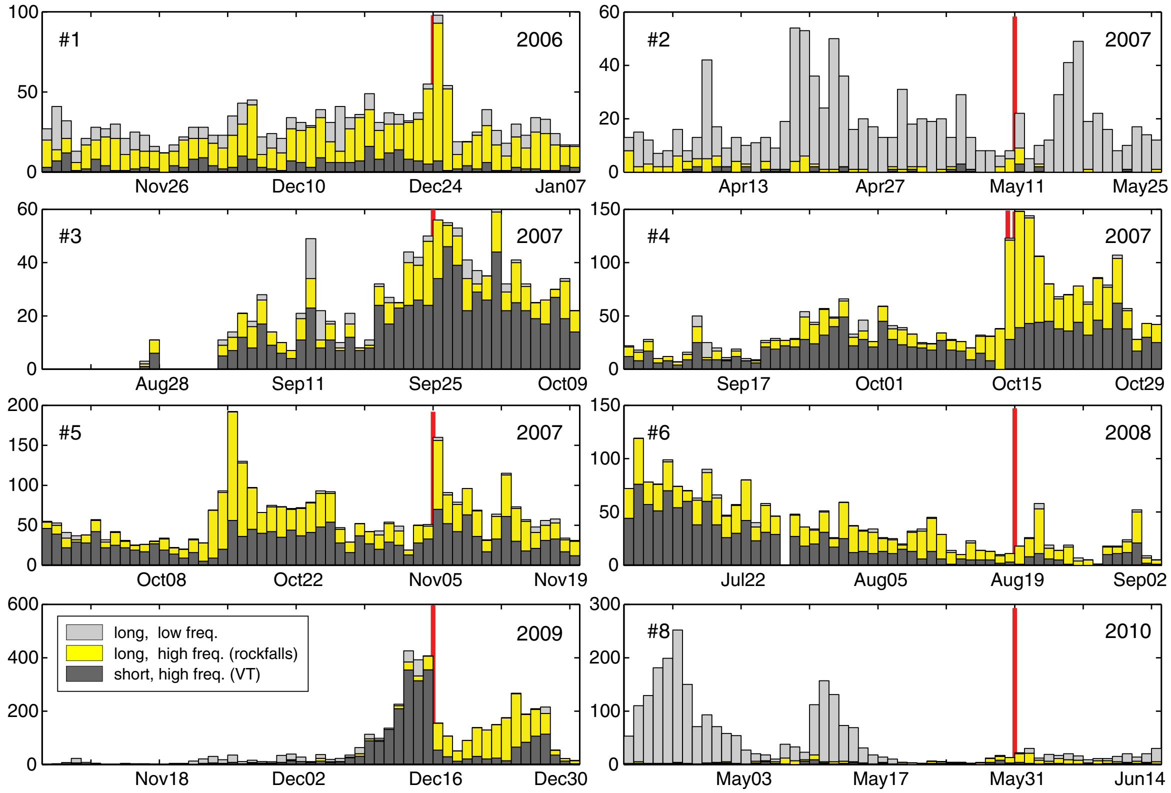

Fig. 7. Daily earthquake rates for each event class in 55-day windows around each eruption. Note that the histogram bars are stacked so as to not obscure each other. The height of the bar represents the total number of events in the given day.

periods as long as 120 s. Eruptions 7 and 8, however, are the only explosions that exhibit this type of seismicity above the noise level.

4. Discussion

4.1. Eruption precursors

Few Bezymianny eruptions have occurred since 2000 without advance activity. The most commonly observed precursors have been increased seismicity and ground temperature thermal anomalies (Ramsey and Dehn, 2004; Senyukov, 2006). These observations underpin the algorithms used operationally to forecast Bezymianny eruptions. The 1956 sector collapse left an amphitheater-like crater open to the southeast. The breach in the crater funnels pyroclastic flows, lahars and surge deposits in roughly the same direction during each eruption (Carter and Ramsey, 2009; Girina, 2013). The forecasting success and this broad similarity of eruption deposits suggest that the mechanics of the eruptions are similarly repeatable. The variety in observations in Section 3 hint that, in fact, several different mechanisms are at work. The challenge is to understand whether these multiple mechanisms coexist randomly or are responses to the same underlying processes.

4.1.1. Precursory tremor

Seismic tremor is a consistent precursor to Bezymianny eruptions (Fig. 3). Six of the eight eruptions show a strong increase in tremor in the day prior to eruption. Eruption 2 does not show a strong tremor signal. However, the background noise level is much higher for this eruption and strong enough to mask the tremor observed during other eruptions. Klyuchevskoy volcano was erupting during this period. Its effusive basaltic eruptions produce powerful tremor in the 1–5 Hz band lasting weeks to months. Though this noise overlaps in frequency, there are indications of Bezymianny's tremor pulsing above the background noise. The other event without a clear tremor precursor is number 5. This event is thought to be a gravity-driven collapse from the dome or the front of the lava flow. Though the deposits from this event stretch ~2 km (Carter and Ramsey, 2009), there are no indications of an explosion at the time. Thelen et al. (2010a) demonstrate that this eruption did not involve the conduit. The absence of notable precursory tremor is consistent with this being a collapse event.

The increase in tremor begins 12–36 h prior to eruptions with an energy increase of two to three orders of magnitude. Comparable changes in energy are not observed outside of eruption periods during the four-year study. The short rise time makes energy particularly useful for forecasting. Several eruptions (1, 6, 7, 8) show a quasi-exponential increase in tremor that effectively points to an eruption time. Though not foolproof, this trend can in theory be modeled to provide an estimate of the eruption time, comparable to Smith and Kilburn (2010). The closer the eruption gets, the more precise the solution could be. An exponential increase in tremor amplitude in the hours preceding eruption is a globally observed phenomenon. In a literature review study, McNutt and Nishimura (2008) find that half of the eruptions in their study have exponentially increasing tremor with durations ranging from 5 min to 63 h. Tremor durations cluster much more tightly at Bezymianny increasing the forecasting potential.

The second pulse of eruption 4 is not preceded by a rise in energy. This is expected since the conduit system had vented 12 h earlier and was presumably still open. No energy was required to prepare the conduit for eruption. This unusual second eruption lasted for a day and appears to have accompanied the extrusion of a viscous lava flow (Carter and Ramsey, 2009) (see Section 4.4).

4.1.2. Precursory seismicity

Earthquakes occur throughout the Klyuchevskoy group of volcanoes. The majority of these occur in the shallow crust beneath Klyuchevskoy volcano and in a very active cluster at 30 km depth (e.g., George, 2010; Thelen et al., 2010a). Fortunately, earthquakes at Bezymianny are

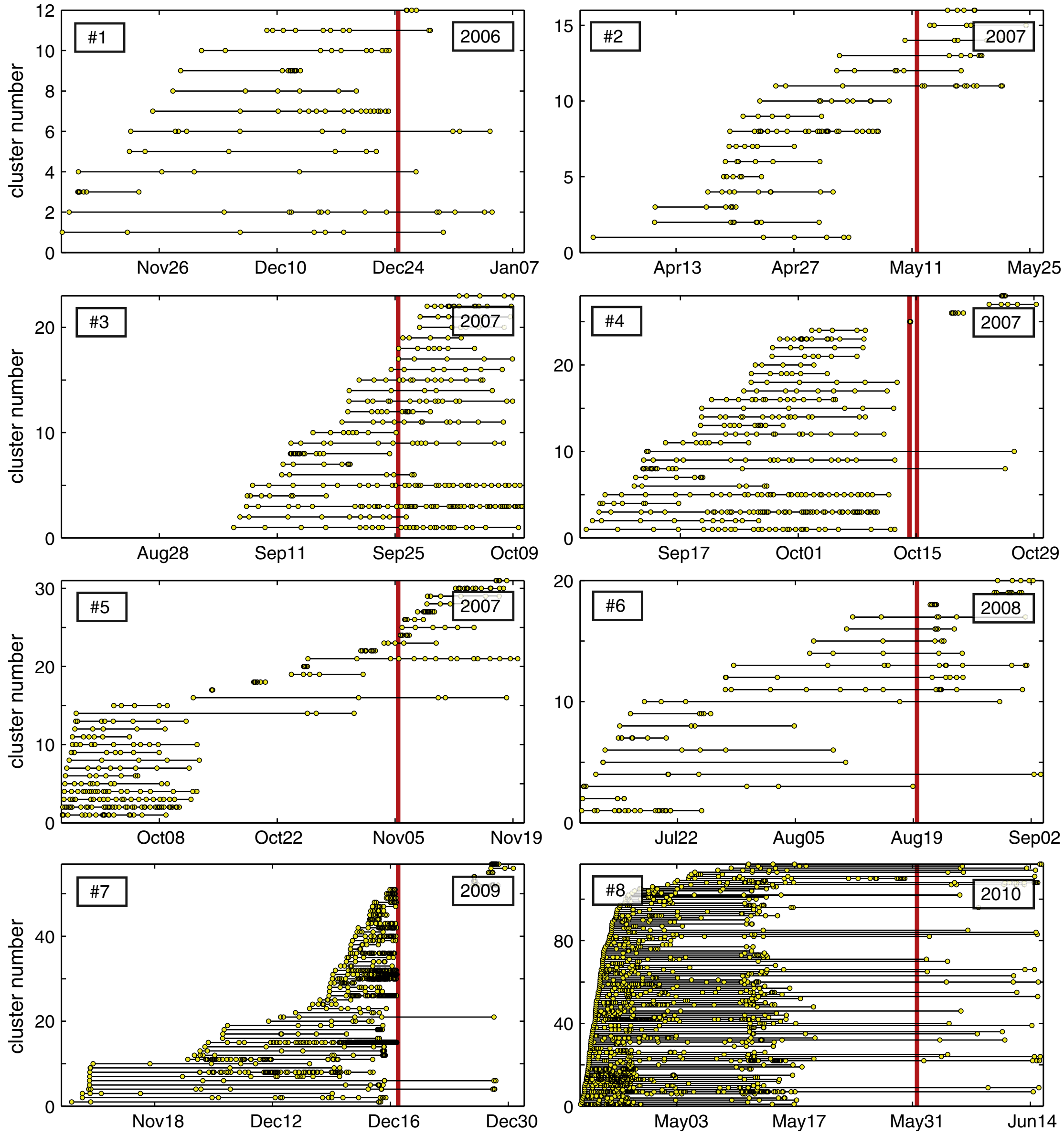

Fig. 8. Multiplet lifespans following Thelen et al. (2010a). Panels span 55 days around each eruption, marked with a red vertical line. Horizontal lines represent the amount of time that a given multiplet was active. See Section 3.6 for explanation.

spatially separated from other clusters. Over the course of the project, the permanent telemetered network was greatly expanded at Bezymianny. As a result, the location errors were cut in half and the magnitude of completeness in the routine earthquake catalog produced by KBGS was improved from about 1.1 to 0.8, as estimated from the hinge point in plots of cumulative occurrence vs. magnitude (not shown).

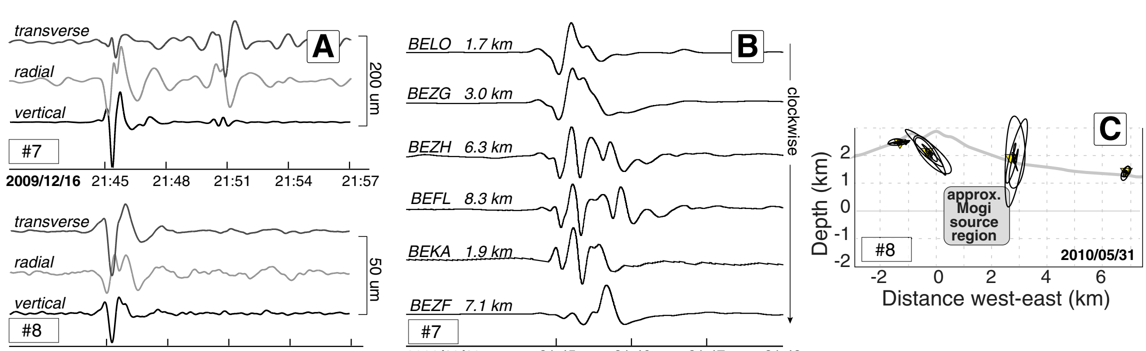

Fig. 9. Very long period co-eruptive seismicity associated with Bezymianny eruptions. Panel A: three-component displacement waveforms for events 7 and 8. Panel B: vertical component records across the network for event 7. Panel C: particle motion cross-section for event 8.

Using earthquakes in the KBGS catalog, eruptions 1 and 7 were preceded by a week of unmistakable seismicity (Fig. 5). Eruption 4 had one day of precursory seismicity. Background noise from Klyuchevskoy obscured seismicity during the build up to eruptions 2 and 8. Overall though, the link between eruptions and advance earthquakes is not as robust as might be anticipated. At volcanoes that have not erupted for several years, explosive eruptions are nearly always preceded by vigorous seismicity (e.g., Moran et al., 2008; Buurman and West, 2010; Ruppert et al., 2011). Thelen et al. (2010b) have demonstrated that the cumulative moment magnitude of precursory seismicity increases with the repose time. In this model, the magnitude of the seismicity reflects how much energy is needed to reopen the conduit, which in turn is determined by how much time the magma has had to cool in place following the previous eruption. On the scale of decades, Thelen et al. (2010b) show that Bezymianny fits this model. Data in Table 1 demonstrate that this model can be applied on the scale of months as well. Precursory cumulative moment magnitudes are based on the week of seismicity preceding each eruption. No data point is available for eruption 2 due to noise from Klyuchevskoy that obscured potential earthquake activity. Event 3 is ignored since it is known not to be a magmatic eruption (Carter and Ramsey, 2009). Fig. 10 shows that the most energetic earthquake swarms precede the eruptions with the longest repose times. While this relationship is not without scatter, it suggests an improved ability to forecast Bezymianny eruptions when the repose time is longer.

The detected seismicity catalog contains events an order of magnitude more than the KBGS catalog. The larger population of events increases the statistical robustness of the event classifications and multiplet analysis, while being more inclusive of rockfalls and low frequency earthquakes. Trends in the high frequency detected seismicity track the KBGS catalog for most eruptions. It appears that the detected seismicity is simply a more inclusive representation of the KBGS catalog. The greater number of small events predicted by the Gutenberg–Richter relationship (Gutenberg and Richter, 1954) suggests that the detected events include the KBGS catalog in addition to events that are smaller by one-half to one magnitude, highly dependent on the *b*-value. While data is insufficient to estimate this exactly, visual inspection of the waveforms and the catalog confirms that small magnitude events comprise the difference between the catalogs.

The clearest pattern in the event classifications is the large number of low frequency events in the time windows around eruptions 2 and 8. These two periods correspond to the strongest tremor activity from neighboring Klyuchevskoy (Fig. 3). Based on this association, I do not consider the low frequency event class, as determined here, to be diagnostic of Bezymianny activity. The low frequency events during the other six eruptions do not demonstrate tractable patterns. However, the low frequency events do provide a valuable way to characterize the seismicity contributions from Klyuchevskoy.

The two classes of high frequency seismicity (VT and rockfall) do show patterns with Bezymianny eruptions. An increase in VT earthquakes precedes some eruptions. Eruption 3 has a steady rise in VT events over a few weeks. A similar pattern is suggested for eruption 1 though the data is weaker. This pattern is most clear for eruption 7. Not only does the rate reach 350 events per day, the increase is also quasi-exponential, suggesting some ability to forecast an eruption time. The network coverage was at its best for eruption 7 suggesting that good data coverage near the crater might have improved the results during other time periods. After eruptions, there is an increase in the rockfall rates. Though this is an expected phenomenon, Fig. 7 demonstrates that increased rockfall activity lasts anywhere from a day (events 1, 5) to two weeks (events 4, 7).

Some eruptions are preceded by increases in rockfall activity (events 1, 4, 7 and possibly 2). This increase in rockfalls has long been observed anecdotally in the field prior to eruptions. The data suggests that it is not ubiquitous, but rather precedes just some eruptions. The variable occurrence of VT and rockfall activity suggests different physical processes occurring before eruptions. Sample waveforms (Fig. 6B) demonstrate that these are notably different types of events. It is challenging to corroborate these observations with the spotty field observations. It is possible that extruded magma spines, thought to precede some eruptions (see Section 1 and Malyshev, 2000), topple from the dome creating these rockfalls. Similar relationships have been noted elsewhere (e.g., Calder et al., 2005). It is also possible that increased gas and heat passing through the dome create instabilities that trigger rockfalls. A final possibility is that the dome expands slightly before eruptions causing the rockfall activity.

4.1.3. Precursory multiplets

The mere occurrence of multiplet seismicity has only modest predictive capability. The author is unaware of significant volcano earthquake sequences anywhere that do not exhibit multiplets. At Bezymianny, multiplet activity appears as a consistent subset of the overall seismicity (see similarities in Figs. 7 and 8). This suggests that high frequency multiplet events exist as a natural part of any large population of volcanic earthquakes. Multiplets do however require a repeatable source and, by extension, a consistent stress regime. The time over which a multiplet is active, referred to here as its lifespan, is a rough proxy for the consistency of the stress patterns. When the stress regime changes, many existing multiplets will cease, possibly followed by new multiplets. In the build-up to an eruption, most multiplets are presumably related to increasing volumes of magma or increasing fluid and gas pressures as a result of fresh magma. Events 1, 3, 4, and 7 have increased multiplet activity in the weeks prior to eruption. I do not consider events 2 and 8, as they appear to be manifestations of the Klyuchevskoy eruption, and not of Bezymianny. The precursory multiplets, like increased seismicity, are suggestive of gradual stress increases in the volcano. Some of these multiplets cease abruptly at eruption (events 1, 4 and 7). As introduced in Thelen et al. (2010b), this cessation indicates that the eruption was sourced deep enough to restructure the stress regime and gas pathways in the conduit. On a practical level, multiplet lifespans present a way to distinguish between eruptions sourced from the surface (such as dome collapses) and those that tap the crustal reservoir. The multiplet lifespans in Fig. 8 demonstrate that events 1, 4 and 7 destroyed the multiplet source, presumably by tapping the volcano at depth. Across events 3 and 5, however, the multiplets are unaffected suggesting that these were surficial events that did not influence the magmatic system. This agrees well with previous speculation that these were dome collapse events.

The multiplet history of eruption 7 is unique. In addition to the large rates, it has two clear multiplet time scales. There is an increase in multiplet activity beginning one week before the eruption. Then

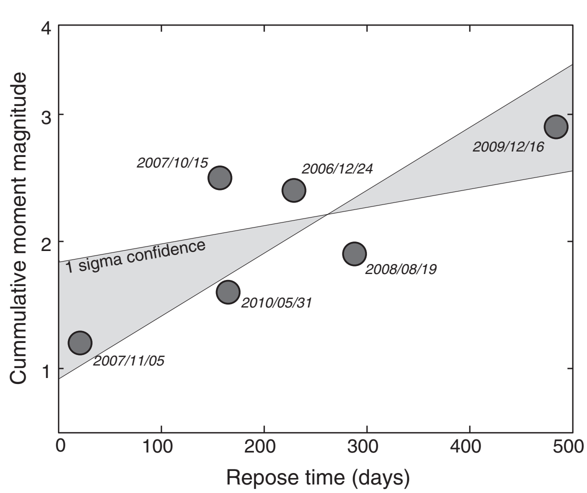

Fig. 10. Repose time vs. cumulative moment magnitude. The shaded region marks the one-sigma error bounds for the best line fit to the data. Though scatter is significant, this plot demonstrates a positive correlation between the two parameters. See Section 4.1.2 for details.

two to three days before the eruption, the number of concurrent multiplets jumps significantly. What is remarkable, however, is that the older multiplets continue to remain active until the eruption. This cannot be explained by ever-changing stresses from, for example, magma rising in the conduit. This would tend to terminate existing multiplets. Instead, it suggests a steady increase of a single stress condition, such as an inflating magma reservoir or a gas system that is not able to vent adequately. These multiplets terminate abruptly with the eruption. Figs. 3 and 6 demonstrate that this is not due to poor event detection. The multiplets truly end. This eruption, more than any other, appears to have destroyed the entire set of multiplet conditions.

4.2. Eruptions

4.2.1. Eruption onsets and durations

Gross parameters contained in information releases and databases suggest that eruptions between 2006 and 2010 are relatively similar (KVERT, 2005–2010; Venzke et al., 2012). Comparable ash cloud heights, recurrence times, deposits and VEI support this. Examination of the spectrograms in Fig. 4 reveals several types of activity, however. Some eruptions begin abruptly. The onset times for events 4, 5 and 7 can be readily determined to better than a minute (Table 1). The remaining eruptions have more gradual onsets. While the slow onset eruptions exhibit dramatic increases in seismic energy, it is less clear which moment in time corresponds to the physical start of the eruption. In contrast, explosive eruptions have, by definition, abrupt onsets. The moment the plug is overcome, the vent clears in a sudden explosive rush.

In contrast, if the conduit is open or only weakly plugged then it is more likely to start with a gradual runaway process than with a sudden explosion. Such a runaway process is inferred when the rate of gas exsolution exceeds the conduit's ability to vent this gas. In situ gas exsolution causes the magma to expand and rise further in the conduit, which triggers further degassing. This positive feedback builds quickly into a full eruption. However, it lacks the singular moment in time when the conduit is catastrophically breached. The two different styles of eruption onset in Fig. 4 suggest that both mechanisms occur at Bezymianny.

Explosive eruptions at Bezymianny are generally short, with high-energy venting lasting less than half an hour, and in some cases, much less (Fig. 4). The eruptions with rapid onsets generally have their peak energy within the first couple of minutes. It is reasonable that their higher explosivity would be front-loaded with energy. The runaway effusion inferred for slow onset eruptions peaks later, once magma has risen further in the conduit and the exsolution process has escalated. A slow onset of seismic energy can also be indicative of large gravity-driven collapses. Pyroclastic flows and lahars have a characteristic cigar-shaped seismic envelope that can last several tens of minutes (Zobin, 2012; Buurman et al., 2013). The Bezymianny lava dome is a well-formed cone reflecting its critical angle of repose. Within a few kilometers of the crater, small rockfalls on the dome are heard almost continuously, even during non-eruptive times. Significant rock avalanches are reported regularly by KVERT (KVERT, 2005–2010) and, at times, can be traced to specific changes in dome morphology (Carter and Ramsey, 2009). The gradual onset and decay of some of the eruptions in Fig. 4 suggest a strong component of dome collapse.

4.2.2. Co-eruptive deformation from VLP seismicity

Most observations of VLP ground motions at periods > 20 s are bursts lasting no more than a couple of minutes and often accompany explosive activity. Representative examples include Popocatepetl (Arciniega-Ceballos et al., 1999), Stromboli (Chouet et al., 2003) and Redoubt (Haney et al., 2013). For volcanoes that have sustained eruption phases, VLP events can persist as a tremor-like signal. Examples of sustained VLP “tremor” include Okmok (Haney, 2010) and Stromboli (De Lauro et al., 2005). These tremor events are typically dominated by energy at the short end of the VLP spectrum (< 10 s), however.

In the current study, so-called very long period seismicity is observed during events 7 and 8 only. The presence of oscillatory VLP signals is an indicator that the edifice had significant co-eruptive cycles of inflation or deflation and recovery. While the absence of VLP signals might be attributable to a number of factors, including source orientation and background noise, events 7 and 8 stand out as unique. Both eruptions produced long period displacements lasting a few minutes and exhibiting periods as long as 120 s. Considerable displacements are seen on all three components. The number of available data channels (and differing station coverage) is poorly suited to the most common approaches to VLP source inversion (Dawson et al., 2011). Three observations are significant here, however. The first is that just two of the eight events produced any distinct VLP signal. The first six eruptions show no evidence of the deflation cycles generally assumed to source co-eruptive VLP signals. This could be because very little mass was actually evacuated from within the volcano, as in the case for a dome collapse. Or it could be because magma and/or volatiles were evacuated at such a slow rate that it did not register within the sensitivity band of the seismic stations. Given the general explosivity of the eruptions, the latter explanation seems unlikely. It is more plausible that the first six eruptions did not tap a deep-seated reservoir and were instead sourced from very high in the edifice.

The second observation is that VLP signals are seen on stations 8 km from the vent (Fig. 9B). Even at this distance, there is significant vertical motion. A shallow source located high in the edifice or in the dome would not generate this type of deformation. If we assume the co-eruptive source had a strong isotropic component (e.g., Waite et al., 2008; Dawson et al., 2011) then the rectilinearity of the particle motions can be used to back project to a very approximate Mogi source region (Mogi, 1958). The dominance of vertical ground motion could indicate a larger vertical component in the source moment, or a single force term not accounted for. Fig. 9C demonstrates the approach. The approximate source location is shallower than the magma inferred from seismicity by Thelen et al. (2010a). However the shallow depth and offset to the east of the summit is in broad agreement with the zone of earthquake activity illustrated by Thelen et al. (2010a).

The third notable observation is that the particle motions are different for each explosion indicating that the source mechanisms were not the same. Data are insufficient to model whether the general types of mechanisms might be the same (e.g., sub-horizontal sill deflation, conduit single force, etc.). However, they do demonstrate that the explosion source in May 2010 was not simply a reactivation of the same source from December 2009.

Eruption 7 is notable because of its two distinct VLP signals separated by 5 min. The different particle motions indicate different source mechanics. The first is associated with the initial explosive eruption unmistakable in the higher frequency data (Fig. 4). The second VLP signal is not distinct in the high frequency explosion record. This could be because the explosion that accompanied it is muffled by the coda of the first explosion. A more likely scenario is that the second VLP was not associated with a distinct magmatic explosion. It could instead be the result of a gas-rich exhalation or perhaps a local response as the ash column collapsed and the surge deposits rushed across the flanks of the volcano. The exact nature of this second VLP is not clear, but is worth keeping in mind when examining similar eruptions elsewhere.

4.3. December 2006 dome collapse

The eruption of December 24, 2006 was the first eruption at Bezymianny to be digitally recorded closer than 15 km. It was also the first broadband record at Bezymianny. The emergent envelope of this first eruption was a surprise because tall ash columns and rapid increases in seismicity typically suggested explosive onsets for recent eruptions. The eruption onset at 09:17 UTC was determined visually (KVERT, 2005–2010). Fig. 11B demonstrates that the ground motion was much stronger 45 min later. This is unlike the other eruptions in

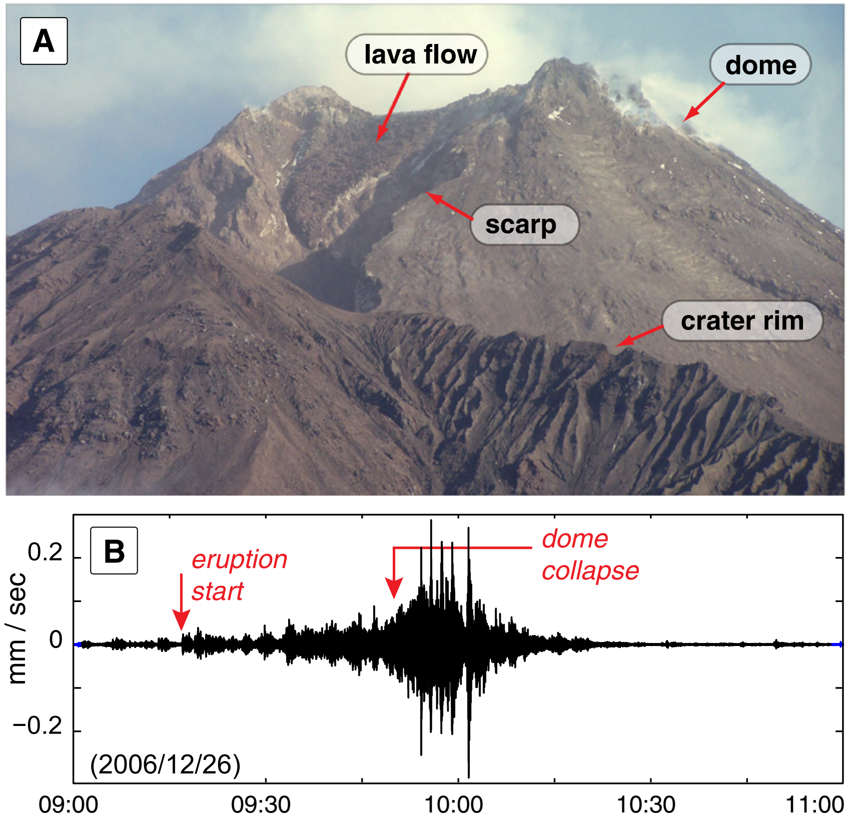

Fig. 11. Details of the December 2006 eruption (event 1). Panel A: photo showing the dome collapse scarp and ensuing lava flow. Panel B: two-hour seismogram illustrating the dome collapse sequence. See Section 4.3 for details.

this study and uncharacteristic of explosive volcanism in general. After 30 min of eruption, the seismic amplitude increases ten-fold over a period of 10 min before decaying over the next 15 to 30 min. The frequency content of this envelope is distributed over a wide band without any clear peaks or dominant frequencies making conduit-sourced tremor an unlikely explanation. There is no evidence of a harmonic or narrow-band signal that would indicate a resonant source, as is typically inferred for tremor sources. The cigar-shaped envelope is more typical of gravity-driven surficial events such as avalanches, pyroclastic flows and lahars. The exact source of this energy remained elusive until the seismic data was reconciled with field observations. At some point during the eruption, a new scarp was created on the south face of the dome (Fig. 11A). This scarp was first recognized in aerial surveillance on December 27 (Girina, 2013). This collapse generated a pyroclastic flow that stretched 6.5 km and was up to half a kilometer wide (Carter et al., 2008). When reconciled with the seismic data, it appears that this collapse began slowly half an hour after the eruption onset and failed progressively over a few tens of minutes. There is no evidence of a singular instantaneous collapse. Photographs show a tongue of high viscosity lava that was extruded into the scarp following the collapse (Carter et al., 2008). The seismic data does not constrain the timing of this lava flow.

It is logical to speculate whether there was any real eruption of juvenile material, or whether this entire event was simply a gravity-driven failure of the dome. The eruption exhibits neither a paroxysmal onset nor VLP signals that might indicate an explosive trigger. Juvenile products are found in the eruption deposits however. In addition, the tremor, earthquakes and multiplet activity show clear eruption precursors. The energy release in the 36 h prior to the eruption follows the same pattern as other eruptions (Fig. 3). Elevated earthquake activity typically precedes eruptions (Fig. 5). And the multiplet activity increases somewhat before terminating at the eruption (Fig. 8). Together these observations indicate that, though it triggered a significant dome collapse, the eruption was ultimately the result of fresh gas and/or magma beneath the edifice.

4.4. October 2007 continuous eruption

Unlike the other eruptions, the event of October 14–15, 2007 was drawn out over more than 24 h. It began with a clear explosive event at 14:27 UTC on October 14. This was a short-lived explosion, not unlike other eruptions in the study. A potential VLP signal is observed on one station at the time of eruption (not shown). Fig. 12A shows a time sequence of AVHRR satellite images processed to maximize ash detection (Prata, 1989). See Webley et al. (2009) for processing and application specifics. The initial cloud is small but with high ash concentration. This corroborates the seismic evidence for a strong short-lived explosion. Tremor in the hours surrounding this eruption follows a typical pattern with a clear ramp-up to the eruption and decay afterwards (Fig. 12B). Twelve hours later, however, the eruption activity resumed with no forewarning. Seismic activity spiked on October 15 at 02:23 UTC. Seismicity remained high and irregular over the next day. The AVHRR images show that ash emission resumed at this time and continued for at least 12 h. No VLP seismicity occurred during this second phase. The multiplet activity in Fig. 8 (and discussed at length in Thelen et al., 2010a) appears to cease with the initial explosive eruption though tremor could be masking these events. Together these observations point toward an initial vent clearing high-pressure eruption with some evidence that the conduit system was involved at depths below the dome (VLP seismicity and multiplet termination). After 12 h, the volcano entered a period of continuous eruption. This is probably due to the steady effusion of gas-rich magma from the reservoir. If gas exsolution was entrapped by viscous magmas, fragmentation in the upper most part of the conduit could drive a sustained ash-rich eruption.

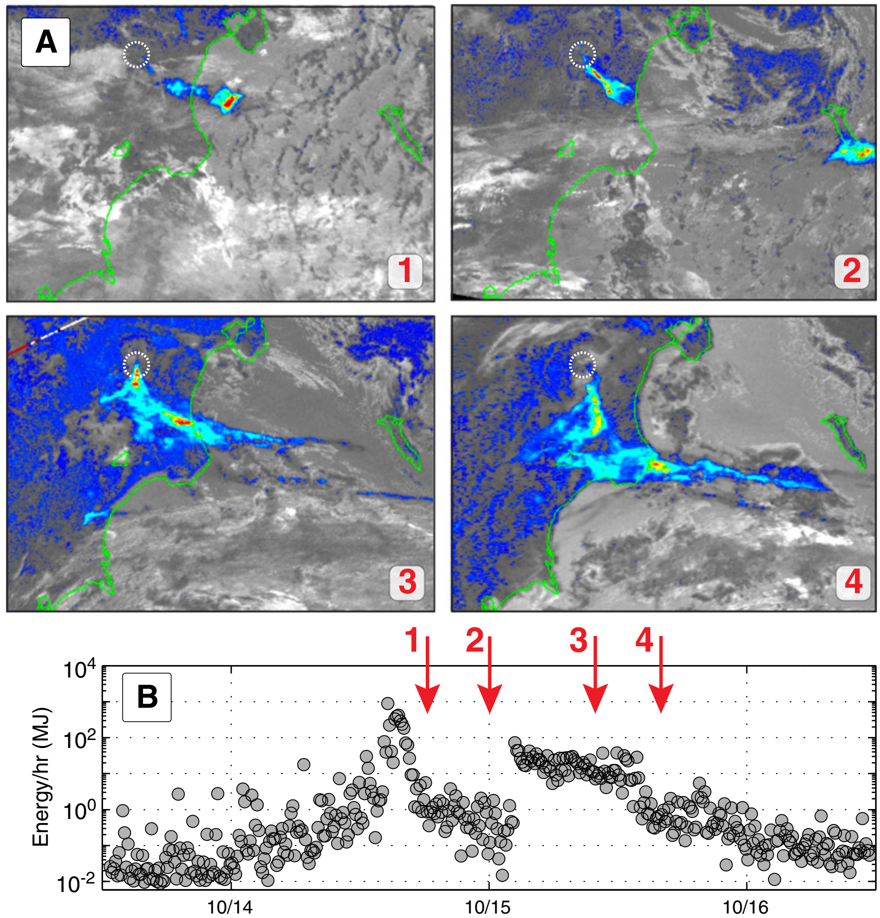

Fig. 12. Comparison of seismic tremor and ash cloud emission during the October 2007 eruption (event 4). Panel A: processed AVHRR images highlighting atmospheric ash concentrations over a 15-hour period. Panel B: tremor amplitudes during this continuous eruption sequence. Red numbers match the image times to the seismic data. See Section 4.4 for details.

This process would have continued until the magma ascent slowed sufficiently to allow gas to vent independent from the magma. At this point, vigorous degassing continued and the magmatic eruption transitioned to lava extrusion. Aerial reconnaissance five days after the eruption revealed a new 400 m long lava flow, confirming this transition (Carter and Ramsey, 2009).

What is interesting about this eruption is the delay between the presumed vent-clearing explosion and the continuous eruption. The initial explosion was probably driven by pressurized gas within vesicular magmas trapped beneath cooled degassed magmas (Sparks, 1997). Though the AVHRR signal demonstrates a strong ash signal associated with this explosion, it is not known whether this was juvenile material or existing dome rock entrained during the explosion. The quiescence following this eruption could be explained by a plug of frozen magma that capped the system again for 12 h. If this were the case, though, I would expect to see the same precursory seismic energy and multiplet activity that precedes other eruptions. These did not occur. A more plausible explanation is that the initial explosion cleared the vent allowing magma to ascend in the conduit and possibly begin effusing. After 12 h, either cooler magma or an increased ascent rate began to prevent gas from escaping the magma. Gas expansion within the magma column caused the magma to fragment and be ejected as a high velocity ash-rich plume.

4.5. December 2009 and May 2010 explosive eruptions

The eruptions of December 2009 and May 2010 stand out from the other eruptions as being significantly more explosive. These two eruptions have the shortest durations and highest releases of seismic energy during the 2006–2010 period (Table 1). Duration and total energy do not sufficiently describe the impulsiveness of these eruptions. Fig. 4 (insets) demonstrates that both of these eruptions began with a pulse of high amplitude energy lasting only seconds. Both have clear precursory tremor in the day preceding eruption. These are also the only two eruptions to exhibit unequivocal VLP signals (Fig. 9A). These observations implicate a conduit system that is plugged, causing gas and gas-rich magma to build up. Webcam observations indicate vigorous steaming preceding these eruptions. Much like an espresso pot that steams vigorously while pressure builds inside, pressure in the conduit system can still be increasing while steaming energetically. During a period of clear weather two days prior to the May 2010 eruption, a vigorous steam plume can be seen extending more than 1500 m above the summit. When the conduit is finally breached, the explosion is instantaneous because substantial gas is already exsolved from the magma and at high elevation in the edifice. The VLP seismicity, inferred in Section 4.2 to be sourced a few kilometers below the summit, is connected to this explosion. The deep VLP deformation begins a matter of seconds after the explosion.

If these eruptions resulted from the sudden release of pent-up gas, then a significant infrasound signal would be expected. No infrasound was being recorded on the volcano at this time, though ground-coupled airwaves are observed on distal seismic stations for the Dec. 2009 eruption (not shown). More significant, however, are the long-distance infrasound recordings. Infrasonic array I44RU is located 370 km to the south–southwest near Petropavlovsk–Kamchatsky. Data from this array, available from the Comprehensive Nuclear-Test-Ban Treaty Organization

(CTBTO), show signals well above the noise for both of these eruptions. December 2009 registers a pressure of 11 Pa (peak-to-peak). The May 2010 signal is 1.5 Pa (pers. comm., D. Fee). Seasonal variations in the array sensitivity are thought to be minimal because the dominant winds are perpendicular to the propagation path. Data from I44RU is only available for two of the events before 2009. Only event 2 shows a detectable signal with an amplitude of 0.17 Pa. The December 2009 pressure pulse was large enough to be recorded 2900 km to the northeast in Fairbanks, Alaska. Two hours and fifty minutes after the eruption, this event registered an amplitude of 0.7 Pa on CTBTO array I53US (pers. comm., D. Fee). While the infrasound data record is not complete for the study period, the evidence agrees with the observation of these two eruptions being substantially more explosive.

Seismic amplitude, infrasound amplitude and total seismic energy mark the December 2009 eruption as five to ten times more energetic than May 2010. The consistent pattern of eruption deposits demonstrated for most eruptions (Girina, 2013) is broken only by the December 2009 eruption. This eruption was the only one during this period to leave significant deposits in the 1956 blast zone east of the dome. Several centimeters of fine-grained deposits at station BERG, as well as displaced rocks, suggest that a pyroclastic surge flowed over the region for this eruption only. While this could have resulted from a different directivity of the eruption, a more likely explanation is that the higher energy eruption produced an ash column that then collapsed to create the surge.

4.6. Future eruptions at Bezymianny

Examining the conceptual model in Fig. 1, there are several possible futures that could unfold at Bezymianny. There is currently little indication that we should expect a return to the steady effusive eruption of the 1960s. Though lava flows have accompanied several recent eruptions, they have been extremely viscous and have shut down within days or a few weeks. Cooler magmas and thorough degassing presumably account for the thick blocky flows. Regardless of cause, however, the high viscosity magmas and their slow extrusion rate suggest that they are not far off from seizing in the conduit and can only be erupted when the vent is periodically re-established by explosions. Another possibility is that Bezymianny could soon return to dormancy. The staccato eruptions of the past few decades could be the final throes of a system that has, morphologically at least, nearly returned to its pre-1956 state. While this must remain a possibility, there is little evidence to suggest an imminent shutdown.

Continued intermittent explosive activity is the remaining option. This is the future of least astonishment and is perhaps not an exciting claim. The pattern of the past two decades has continued while this manuscript was being prepared, however, and there are few lines of reasoning that can argue for a drastic change in activity. Even so, the potential of indefinite explosive eruptions is a future with real consequences. Ash fall from current eruptions impact several communities in the area, including Klyuchi and Kozyrevsk. Fortunately, most are

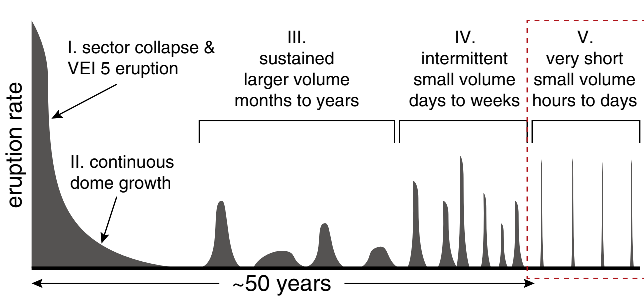

Fig. 13. Version of Fig. 1 modified to characterize proposed recent and future eruptive activity. This conceptual model projects shorter-lived, but somewhat more explosive, eruptions. See Section 4.6 for full explanation.

relatively resilient to frequent ash and are beyond the reach of pyroclastic flows. Bezymianny and the Klyuchevskoy group of volcanoes have also become important tourist destinations. In the summer months, tourist groups are regularly camped on the flanks of Bezymianny for extended periods of time. In mid-July 2008, a month before eruption 6, groups were evacuated from Bezymianny when a sudden increase in seismicity (Fig. 5) was accompanied by hot rock avalanches that flowed 5 km from the dome down the same southeast chute followed by recent pyroclastic flows (see Girina, 2013, Fig. 2). The hazards from Bezymianny reach far beyond Kamchatka though. Ash rich eruption clouds ascend directly into primary flight paths between Asia and North America (Neal et al., 2009). The dominant winds carry this ash eastward, parallel to flight paths and into U.S. airspace (e.g., Fig. 12A). This ash can remain a threat for several days.

Because Bezymianny is remote and because North Pacific weather is often uncooperative, geophysical monitoring and satellite-based monitoring are unusually important. Several of the eruptions discussed in this paper occurred without any direct observation. The first photographs of some of these events were taken days after the eruptions had ceased, when weather permitted observation flights. The combination of high volcanic hazard and the dependence on geophysical monitoring makes the specific patterns of precursors and eruption behavior vital to accurate monitoring—arguably more so than in some locations.

Continued explosive eruptions could follow several patterns. The size of eruptions and the intervals between eruptions could diminish or grow larger. The varied eruption styles observed in recent years could continue, or the eruptions could become more repeatable. The patterns of precursory activity (tremor, multiplet earthquakes, thermal anomalies) could fade or grow stronger. Definitive answers to these questions won't be known until the eruptions occur. Some observations, however, suggest that eruptions could become more intermittent and more explosive (Fig. 13). Lava flows over the past two decades have become short-lived occurrences. Throughout the 1980s, effusive eruptions frequently lasted months or years (Girina, 2013). The quiescence between eruptions was often shorter than the eruptions themselves. This type of activity has not occurred in the past decade. Though significant lava flows have been emplaced as recently as 2010, these periods of effusion lasted just days before the conduit presumably froze again. The eruptions presented in this paper show a modest trend toward increasing explosivity. Eruptions 7 and 8 have multiple indicators that demonstrate higher energy. This trend appears to be continuing after 2010. The possibility of increased explosivity is consistent with the longer repose time between eruptions. Longer repose periods between eruptions allow the conduit system to cool, creating colder, dense, crystal-rich plugs that must be overcome during the next eruption. This fact is substantiated by the higher precursory seismic activity that accompanies longer repose periods (Fig. 10 and Table 1).

The possibility of increasingly explosive eruptions is not immediately welcomed from a monitoring perspective. Larger explosions push ash more quickly into the atmosphere. They also generate more dangerous projectiles. There is potentially a positive note, however, to this speculation. Evidence presented here demonstrates that the most explosive eruptions have the strongest precursors. The high-pressure build-up that drives explosions is also responsible for several precursors. High seismic activity is seen prior to the most explosive eruptions (Fig. 5). The potential of strong multiplet activity as a manifestation of gas pressure is particularly intriguing (Fig. 8). While discussions about future eruptive behavior are clearly speculative, it is promising that these eruptions may also be the most predictable.

Acknowledgments

This study would not be possible without the tireless efforts of dozens of people who made the PIRE field project a success. I dare not attempt to list them all here. Pavel Izbekov taught me that extraordinary things are quite common in Russia. Weston Thelen was a long-term presence both in the field and scientifically. Helena Buurman was a field leader extraordinaire. Silvio De Angelis and Glenn Thompson contributed to this study through numerous discussions and technique refinements. Victor Chebrov, Sergey Senyukov and Dima Droznin at the Kamchatka Branch of Geophysical Services provided countless types of assistance as well as camaraderie. David Fee provided help in accessing the IMS infrasound data. All analysis was carried out using the GISMO seismic toolbox for Matlab (http://code.google.com/p/gismotools), paired with Antelope Environmental Data Collection Software (www.brtt.com). This project was supported under the U.S. National Science Foundation award number 0530278. The seismic waveform data is archived and publicly available at the IRIS Data Management Center.

References

Aki, K., Koyanagi, R., 1981. Deep volcanic tremor and magma ascent mechanism under Kilauea, Hawaii. Journal of Geophysical Research 86, 7095–7109.

Arciniega-Ceballos, A., Chouet, B.A., Dawson, P., 1999. Very long-period signals associated with vulcanian explosions at Popocatepetl Volcano, Mexico Alejandra. Geophysical Research Letters 26, 3013–3016.

Belousov, A.B., Voight, B., Belousova, M., 2007. Directed blasts and blast-generated pyroclastic density currents: a comparison of the Bezymianny 1956, Mount St Helens 1980, and Soufrière Hills, Montserrat 1997 eruptions and deposits. Bulletin of Volcanology 69, 701–740.

Bogoyavlenskaya, G.E., Braitseva, O.A., Melekestsev, I.V., Kiriyanov, V.Y., Dan Miller, C., 1985. Catastrophic eruptions of the directed-blast type at Mount St. Helens, Bezymianny and Shiveluch volcanoes. Journal of Geodynamics 3, 189–218.

Bogoyavlenskaya, G.E., Braitseva, O.A., Melekestsev, I.V., Maksimov, A.P., Ivanov, B.V., 1991. Bezymianny volcano. In: S.A., F., Yu, P., M. (Eds.), Active Volcanoes of Kamchatka, pp. 195–197.

Buurman, H., West, M.E., 2010. Seismic precursors to volcanic explosions during the 2006 eruption of Augustine volcano. In: Power, J.A., Coombs, M.L., Freymueller, J.T. (Eds.), The 2006 Eruption of Augustine Volcano, Alaska: U.S. Geological Survey Professional Paper, 1769, pp. 41–57.

Buurman, H., West, M.E., Thompson, G., 2013. The seismicity of the 2009 Redoubt eruption. Journal of Volcanology and Geothermal Research 259, 16–30.

Calder, E.S., Cortés, J.A., Palma, J.L., Luckett, R., 2005. Probabilistic analysis of rockfall frequencies during an andesite lava dome eruption: the Soufrière Hills Volcano, Montserrat. Geophysical Research Letters 32, 5–8.

Carter, A.J., Ramsey, M.S., 2009. ASTER- and field-based observations at Bezymianny Volcano: focus on the 11 May 2007 pyroclastic flow deposit. Remote Sensing of Environment 113, 2142–2151.

Carter, A.J., Ramsey, M.S., Belousov, A.B., 2007. Detection of a new summit crater on Bezymianny Volcano lava dome: satellite and field-based thermal data. Bulletin of Volcanology 69, 811–815.

Carter, A.J., Girina, O., Ramsey, M.S., Demyanchuk, Y.V., 2008. ASTER and field observations of the 24 December 2006 eruption of Bezymianny Volcano, Russia. Remote Sensing of Environment 112, 2569–2577.

Chouet, B.A., 1996. Long-period volcano seismicity: its source and use in eruption forecasting. Nature 380, 309–316.

Chouet, B.A., Dawson, P., Ohminato, T., Martini, M., Saccorotti, G., Giudicepietro, F., Luca, G.D., Milana, G., Scarpa, R., 2003. Source mechanisms of explosions at Stromboli Volcano, Italy, determined from moment-tensor inversions of very-long-period data. Journal of Geophysical Research 108, 2019.

Dawson, P.B., Chouet, B.A., Power, J., 2011. Determining the seismic source mechanism and location for an explosive eruption with limited observational data: Augustine Volcano, Alaska. Geophysical Research Letters 38, 1–5.

De Lauro, E., Martino, S.D., Falanga, M., Palo, M., Scarpa, R., 2005. Evidence of VLP volcanic tremor in the band [0.2–0.5] Hz at Stromboli volcano, Italy. Geophysical Research Letters 32, L17303.

Del Pezzo, E., Bianco, F., Saccorotti, G., 2001. Separation of intrinsic and scattering Q for volcanic tremor: an application to Etna and Masaya volcanoes. Geophysical Research Letters 28, 3083.

DeRoin, N., McNutt, S.R., Sentman, D.D., Reyes, C., 2012. Seismicity of block-and-ash flows occurring during the 2006 eruption of Augustine Volcano, Alaska. Journal of Volcanology and Geothermal Research 213–214, 14–26.

Droznin, D.V., Droznina, S.Y., 2011. Interactive DIMAS program for processing seismic signals. Seismic Instruments 47, 215–224.

Endo, E.T., Murray, T., 1991. Real-time seismic amplitude measurement (RSAM): a volcano monitoring and prediction tool. Bulletin of Volcanology 53, 533–545.

Fedotov, S.A., 1972. Energy Classification of Kamchatkan Earthquakes and the Problem of Magnitudes. Nauka, Moscow.

George, O., 2010. Relating magmatic processes to eruptive behavior at arc volcanoes through an analysis of deep seismicity. M.S. Thesis, Univ. Alaska Fairbanks. Fairbanks, Alaska.

Girina, O., 2013. Chronology of Bezymianny Volcano activity, 1956–2010. Journal of Volcanology and Geothermal Research 263, 21–40.

Gorshkov, G.S., 1959. Gigantic eruption of the volcano Bezymianny. Bulletin Volcanologique 20, 77–109.

Gusev, A.A., 1991. Intermagnitude relationships and asperity statistics. Pure and Applied Geophysics 136, 515–527.

Gutenberg, B., Richter, C.F., 1954. Seismicity of the Earth and Associated Phenomena, 2nd ed. Princeton University Press, Princeton, NJ.

Haney, M.M., 2010. Location and mechanism of very long period tremor during the 2008 eruption of Okmok Volcano from interstation arrival times. Journal of Geophysical Research 115, 1–13.

Haney, M.M., Chouet, B.A., Dawson, P.B., Power, J.A., 2013. Source characterization for an explosion during the 2009 eruption of Redoubt Volcano from very-long-period seismic waves. Journal of Volcanology and Geothermal Research 259, 77–78.

Johnson, J.B., Aster, R.C., 2005. Relative partitioning of acoustic and seismic energy during Strombolian eruptions. Journal of Volcanology and Geothermal Research 148, 334–354.

Koulakov, I., Gordeev, E.I., Dobretsov, N.L., Vernikovsky, V.A., Senyukov, S.L., Jakovlev, A., 2011. Feeding volcanoes of the Kluchevskoy group from the results of local earthquake tomography. Geophysical Research Letters 38, L09305.

KVERT, 2005–2010. Kamchatkan and Northern Kuriles volcanic activity daily information releases. http://www.kscnet.ru/ivs/kvert/updates.php (Petropavlovsk-Kamchatsky. Last accessed May 10, 2012).

Luckett, R.R., Loughlin, S.C., De Angelis, S., Ryan, G., 2008. Volcanic seismicity at Montserrat, a comparison between the 2005 dome growth episode and earlier dome growth. Journal of Volcanology and Geothermal Research 135, 127–146.

Malyshev, A.I., 2000. The Life of Volcano. Publishing House of Urals Branch of RAS, Ekaterinburg.

McGimsey, R.G., Neal, C.A., Dixon, J.P., Malik, N., Chibisova, M., 2011. 2007 volcanic activity in Alaska, Kamchatka, and the Kurile Islands: summary of events and response of the Alaska Volcano Observatory. U.S. Geological Survey Scientific Investigations Report 2010–5242, 110.

McNutt, S.R., 2002. Volcano seismology and monitoring for eruptions. International Handbook of Earthquake and Engineering Seismology, vol. 81A, pp. 383–406.

McNutt, S.R., Nishimura, T., 2008. Volcanic tremor during eruptions: temporal characteristics, scaling and constraints on conduit size and processes. Journal of Volcanology and Geothermal Research 178, 10–18.

Mogi, K., 1958. Relations between the eruptions of various volcanoes and the deformations of the ground surfaces around them. Bulletin of the Earthquake Research Institute 36, 99–134.

Moran, S.C., Malone, S.D., Qamar, A.I., Thelen, W., Wright, A.K., Caplan-Auerbach, J., 2008. Seismicity associated with renewed dome-building at Mount St. Helens, 2004–2005. In: Sherrod, David R., Scott, W.E., Stauffer, P.H. (Eds.), A Volcano Rekindled: The Renewed Eruption of Mount St. Helens, 2004–2006: U.S. Geological Survey Professional Paper, 1750, pp. 27–60.

Neal, C.A., Girina, O., Senyukov, S.L., Rybin, A., Osiensky, J., Izbekov, P., Ferguson, G., 2009. Russian eruption warning systems for aviation. Natural Hazards 51, 245–262.

Neal, C.A., McGimsey, R.G., Dixon, J.P., Cameron, C.E., Nuzhaev, A.A., Chibisova, M., 2011. 2008 volcanic activity in Alaska, Kamchatka, and the Kurile Islands: summary of events and response of the Alaska Volcano Observatory. U.S. Geological Survey Scientific Investigations Report 2010–5243, 94.

Newhall, C.G., Self, S., 1982. The volcanic explosivity index (VEI): an estimate of explosive magnitude for historical volcanism. Journal of Geophysical Research 87, 1231–1238.

Prata, A.J., 1989. Infrared radiative transfer calculations for volcanic ash clouds. Geophysical Research Letters 16, 1293.

Ramsey, M., Dehn, J., 2004. Spaceborne observations of the 2000 Bezymianny, Kamchatka eruption: the integration of high-resolution ASTER data into near real-time monitoring using AVHRR. Journal of Volcanology and Geothermal Research 135, 127–146.

Rowe, C.A., Thurber, C.H., White, R.A., 2004. Dome growth behavior at Soufriere Hills Volcano, Montserrat, revealed by relocation of volcanic event swarms, 1995–1996. Journal of Volcanology and Geothermal Research 134, 199–221.

Ruppert, N.A., Prejean, S., Hansen, R.A., 2011. Seismic swarm associated with the 2008 eruption of Kasatochi Volcano, Alaska: earthquake locations and source parameters. Journal of Geophysical Research 116, B00B07.

Schneider, D.J., Dean, K.G., Dehn, J., Miller, T.P., Kiriyanov, V.Y., 2000. Monitoring and analyses of volcanic activity using remote sensing data at study for Kamchatka, Russia, December 1997. In: Mouginis-Mark, P.J., Crisp, J.A., Fink, J.H. (Eds.), Monograph. Am. Geophys. Union, Washington, D.C., pp. 65–86.

Senyukov, S.L., 2006. Monitoring of volcanic activity in Kamchatka by remote sensing techniques in 2000–2004. Volcanology and Seismology 3, 1–11.

Senyukov, S.L., Droznina, S.Y., Nuzdina, I.N., Garbuzova, V.T., Droznin, D.V., Kozevnikova, T.Y., 2004. Sheveluch and Bezymianny volcanoes activity investigations in 2000–2003 using remote sensing, integrated seismological and geophysical studies of Kamchatka. Integrated Seismological and Geophysical Studies of Kamchatka. Kamchatkan Methodical Seismological Department. Geophysical Service, RAS, Petropavlovsk-Kamchatsky, pp. 301–318.

Smith, R., Kilburn, C.R.J., 2010. Forecasting eruptions after long repose intervals from accelerating rates of rock fracture: the June 1991 eruption of Mount Pinatubo, Philippines. Journal of Volcanology and Geothermal Research 191, 129–136.

Sparks, R.S.J., 1997. Causes and consequences of pressurisation in lava dome eruptions. Earth and Planetary Science Letters 150, 177–189.

Thelen, W., West, M.E., Senyukov, S., 2010a. Seismic characterization of the fall 2007 eruptive sequence at Bezymianny Volcano, Russia. Journal of Volcanology and Geothermal Research 194, 201–213.

Thelen, W., Malone, S.D., West, M.E., 2010b. Repose time and cumulative moment magnitude: a new tool for forecasting eruptions? Geophysical Research Letters 37, 1–5 http://dx.doi.org/10.1029/2010GL044194.

Thelen, W., Malone, S., West, M.E., 2011. Multiplets: their behavior and utility at dacitic and andesitic volcanic centers. Journal of Geophysical Research 116, B08210 http://dx.doi.org/10.1029/2010JB007924.

Thompson, G., 2011. Optimizing detection of earthquakes swarms in the presence of noise, using Antelope. Internal report, Alaska Volcano Observatory. http://www.aeic.alaska.edu/Input/glenn/reports.php (Last accessed November 2, 2012).

Thompson, G., West, M.E., 2010. Real-time detection of earthquake swarms at Redoubt Volcano, 2009. Seismological Research Letters 81, 505–513.

Trifunac, M.D., Brady, A.G., 1975. A study on the duration of strong earthquake ground motion. Bulletin of the Seismological Society of America 65, 581–626.

van Manen, S.M., Dehn, J., West, M.E., Blake, S., Rothery, D.A., 2010. Combined analyses of thermal satellite data and reduced displacement. In: Power, J.A., Coombs, M.L., Freymueller, J.T. (Eds.), The 2006 Eruption of Augustine Volcano, Alaska: U.S. Geological Survey Professional Paper, 1769, pp. 553–567.

Venzke, E., Wunderman, R.W., McClelland, L., Simkin, T., Luhr, J.F., Siebert, L., Sennert, S., Mayberry, G., 2012. Global volcanism, 1968 to the present. Smithsonian Institution, Global Volcanism Program Digital Information Series, GVP-4. http://www.volcano.si.edu/reports. (Last accessed May 10, 2012).

Voight, B., Glicken, H., Janda, R.J., Douglass, P.M., 1981. Catastrophic rockslide-avalanche of May 18. In: Lipman, P.W., Mullineaux, D.R. (Eds.), The 1980 Eruptions of Mount St. Helens, Washington: U.S. Geological Survey Professional Paper, 1250, pp. 347–378.

Waite, G.P., Chouet, B.A., Dawson, P.B., 2008. Eruption dynamics at Mount St. Helens imaged from broadband seismic waveforms: interaction of the shallow magmatic and hydrothermal systems. Journal of Geophysical Research 113, B02305 http://dx.doi.org/10.1029/2007JB005259.

Webley, P.W., Dehn, J., Lovick, J., Dean, K.G., Bailey, J.E., Valcic, L., 2009. Near-real-time volcanic ash cloud detection: experiences from the Alaska Volcano Observatory. Journal of Volcanology and Geothermal Research 186, 79–90.

Wiens, D.A., Pozgay, S.H., Shore, P.J., Sauter, A.W., White, R.A., 2005. Tilt recorded by a portable broadband seismograph: the 2003 eruption of Anatahan Volcano, Mariana Islands. Geophysical Research Letters 32, L18305 http://dx.doi.org/10.1029/2005GL023369.

Zobin, V.M., 2012. Introduction to Volcanic Seismology, Second edition. Elsevier.